Journal of Applied Science and Engineering, Vol. 16, No. 4, pp. 345–351 (2013) DOI: 10.6180/jase.2013.16.4.02

Small Horizontal-Axis Wind Turbine Blade for Low Wind Speed Operation

P. Pathike, T. Katpradit, P. Terdtoon and P. Sakulchangsatjatai

Department of Mechanical Engineering, Faculty of Engineering, Chiang Mai University, Thailand 50200

Abstract

At low wind speed, modern commercial wind turbines have low efficiency for electricity generation. This research hence aims to design a new small wind turbine blade that is suitable for practical applications. Higher torque has to be obtained properly to generate electricity. In order to design and evaluate performance, our mechanical model has been developed based on Blade Element Momentum theory. And, the model is consequently employed to determine the optimized blade shape with the rotor diameter of the wind turbine no higher than 3 m, a design wind velocity of 6 m/s, using 12 V and 24 V battery chargers. The new wind turbine blade has been manually made from fiberglass (GRP) with safety factors of 4 (for 12 V battery) and 2.8 (for 24 V battery). Experimental study is conducted by testing both the commercial blade and our new blade with a specific wind turbine set. It is found that, at designed wind velocity, the efficiency of the novel wind turbine blade of 27% is obtained while that of the commercial wind turbine is only 16%.

Key Words: Small Wind Turbine, Low Wind Speed Wind Turbine, Wind Turbine Blade, Blade Shape Design

1. Introduction

In Thailand, there is a low potential of yielding wind energy [1] especially in the well-known location of Chiang Mai [2] where the average wind velocity is only 6 m/s. Hence, extraction of energy from wind is mostly obtained by using small wind turbines in order to locally produce electrical energy. Based on power output, small wind turbines can be divided into three categories: micro (< 1 kW, R < 1.5 m); mid-range (1 kW–20 kW, R ≈ 1.5 m–5 m); and mini (20 kW−50 kW, R ≈ 5 m+) [3]. But, modern commercial wind turbines have been designed for suitable use with wind velocity of 8–15 m/s. And in such an environment, their components are fixed and cannot be adapted to their varied environmental conditions, thus, they cannot operate at their highest efficiencies. Although efficiency can be improved by increasing wind turbine blade length to generate electricity, the overall size of turbine will also increase and construction cost will be higher. This dilemma is always encountered in the application aspect of wind energy. Thus, it is better to improve by increasing the torque of the wind turbine. This research consequently attempts to develop a simulation of both wind turbine efficiency and higher torque. The simulation is based on the Blade Element Momentum theory (BEM) which is a classical method to calculate the induced velocities on the wind turbine blade and employed to determine the optimized parameters [4]. Airfoil shape is modified to improve lift force and consequently torque at low wind speed condition [5]. In the analysis and design of our new wind turbine, construction is made less complex while not affecting the generated electrical capacity.

2. Methodology

The designing methodology of wind turbine blades

*Corresponding author. E-mail: phrut@eng.cmu.ac.th

can be mainly divided into three parts; establishment of a mathematical model to predict the operating performance, determination of blade parameters, and experiments for wind turbine blade operating.

2.1 Mathematical Model

The mathematical model to design wind turbines is based on the Blade Element Momentum Theory (BEM) [4]. The axial force (F_N) and torque (T) acting on the blades are as follows:

$$dF_N = B\frac{1}{2}\rho V_0^2 \frac{(1-a)^2}{\sin^2\varphi}(C_L\cos\varphi + C_D\sin\varphi)cdr \quad (1)$$

$$dT = B\frac{1}{2}\rho V_0 \frac{(1-a)}{\sin\varphi}\frac{\omega r(1+a')}{\cos\varphi}(C_L\sin\varphi - C_D\cos\varphi)rcdr \quad (2)$$

Moreover, parameter of induction factors can be calculated by using the following equations:

$$a = \frac{1}{\left[\dfrac{4F\sin^2\phi}{\dfrac{Bc}{2\pi r}(C_L\cos\phi + C_D\sin\phi)}\right]+1} \quad (3)$$

$$a' = \frac{1}{2}\left(\sqrt{1+\frac{4}{\lambda^2}a(1-a)} - 1\right) \quad (4)$$

A new empirical relationship between thrust coefficient and induction factor in the case that axial induction factors are greater than 0.4 has been established [6]. The BEM theory does not yield reliable results in this range of induction factor. In this case, parameter of induction factor, a, can be calculated by using the following equation:

$$a = \frac{18F - 20 - 3\sqrt{C_N(50-36F) + 12F(3F-4)}}{36F - 50} \quad (5)$$

where F is tip loss factor which is defined as following [4].

$$F = (2/\pi)\arccos\left(\exp\left\{-\left(\frac{B(R-r)}{2r\sin(\theta)}\right)\right\}\right) \quad (6)$$

At any local radius r, the combined effect of tensile stress and bending stress can be obtained from:

$$\sigma(r)_{\max} = \frac{F_c}{A} + \frac{M_t d_a}{I_a} + \frac{M_t d_b}{I_b} \quad (7)$$

In this study, the net savings function form is adopted to evaluate and optimize decisions on blade shape selection [7] as follows:

$$N_S = C_P HP - C_{windturbine} \quad (8)$$

Expansion for the net saving function form yields:

$$N_s = \frac{year}{1+d}C_P HQ - [1 - R_v(1+d)^{-year}](C_{windturbine\_set} + C_{windturbine\_blade}) \quad (9)$$

$$C_{windturbine\_blade} = R\left[C_{blade\_casting}B + C_{blade\_mold}B_{chord}B_{twist} + \frac{C_{blade\_root}}{R} + C_{Coating}\right] \quad (10)$$

Efficiency of a wind turbine can be calculated by following:

$$\eta = \frac{P}{\frac{1}{2}\rho A V^3} \quad (11)$$

Steps for engineering problem solving are shown in Figure 1. Input parameters for designing a new wind turbine are explained in next section.

2.2 Specifications of the Wind Turbine

2.2.1 Rotational Speeds

Rotational speed of the electric generator shaft is proportional to electric potential (or voltage). Experimental data of the generator (model FD2.7-500 provided by the Engineo Co., Ltd. [8]) is shown in Figure 2. Thus, in case of the battery charger with 12 V and 24 V electric potential, the operating rotational speed of the electric generator shaft is 100 ± 5 rpm and 180 ± 5 rpm respectively.

2.2.2 Airfoil

Aerodynamic forces (Lift and drag force) are pri-

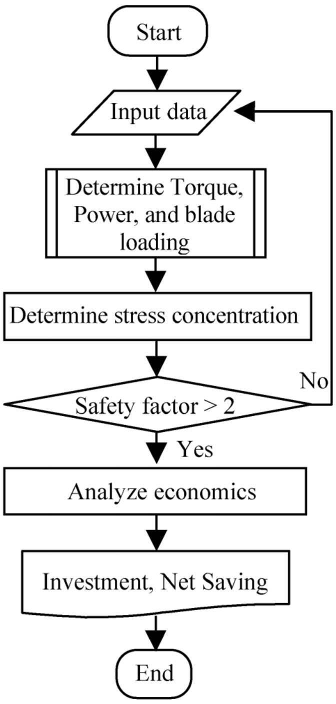

Figure 1. Flow chart of simulation.

marily the result of its airfoil geometry and the angle of attack (α) which is the angle between the chord (c) and the direct of the flow. High ratio of C_L/C_D results in a higher power coefficient of the rotor. According to previous studies [5], airfoil of the FD2.7-500 wind turbine blade's geometry has been developed with its maximum camber, airfoil thickness and their position. For low wind speed, C_L is improved by 10% while high C_L/C_D can still be obtained. Although this airfoil has been tested in a wind tunnel with smaller analogous geometry, in the test it is constructed using an analogous larger size than is used in the actual wind turbine according to reduced wind speed, in order to maintain low wind speed conditions (Re = 60,000). In this study, the improving

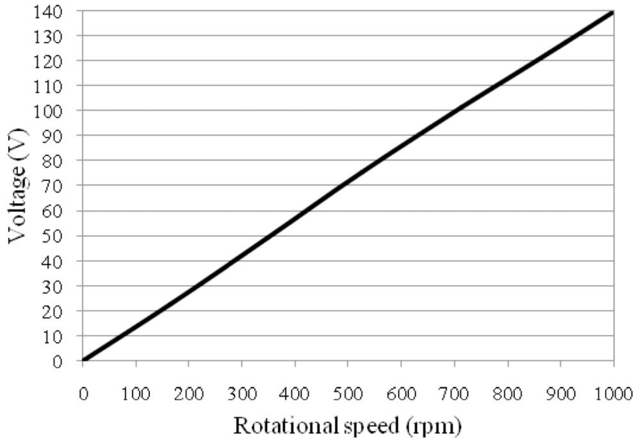

Figure 2. Testing data of generator of FD2.7-500.

airfoil is applied and assumed to be constant along the blade. The airfoil profile and experimental data are shown in Figure 3.

2.2.3 Blade Parameters

Since there are many parameters especially in small wind turbines, we have to identify the appropriate range of all of them to design for the low wind speed range. We will refer to the size of our wind turbine in terms used with commercial small wind turbines. The basic specifications of the turbine are listed as shown in Figure 4. Additional pitch is the pitch angle which is varied according to blade length (Tip position = 20) and there are five twist styles (S) in this study. Hence, overall pitch of each position along the blade length is a combination of the setting angle at the tip section and the additional pitch.

2.2.4 Root Section

Generally, the maximum concentration stresses on a wind turbine blade occur from the bending moment. In the region of extractable power of a wind turbine blade,

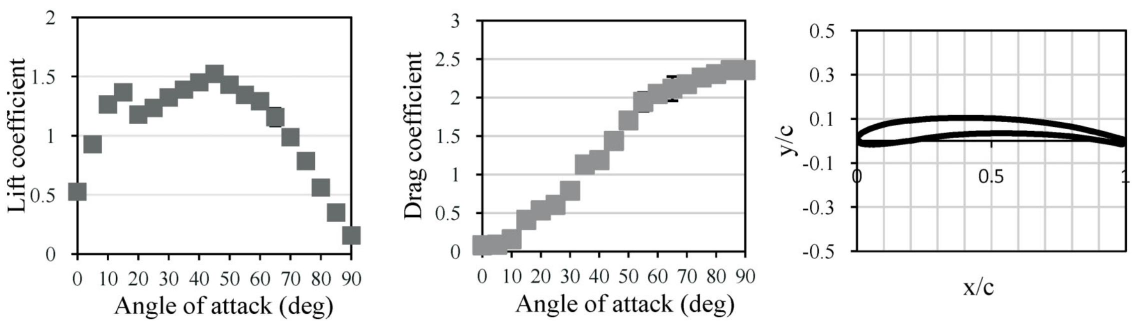

Figure 3. Aerodynamic coefficients and airfoil profile.

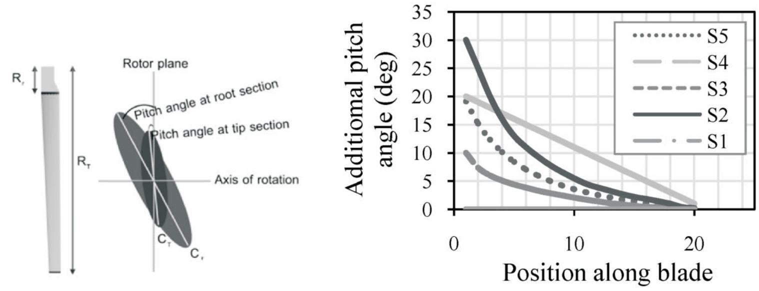

R_{tip} = 0.8 -1.5 m
R_{root} = 0.05-0.15 m
C_{tip} = 0.05 -0.15m
C_{root} = 0.05 -0.15m
B = 3-6
Setting angle at tip section = 0-30°
Twist style =S1-S5
V = 6 m/s
ω = 100, 180 rpm

Figure 4. Rotor parameters.

blade shape cannot be modified to support loading. In this region where wind speed is 12 m/s (Maximum operating wind speed), the safety factor of 2 is adopted for the material of blade support according to the mechanical properties of Fiberglass Reinforced Plastic (GRP) [9] of the design especially during extreme operating situations. Therefore, in the case of stress analysis, root section, which will be connected to the hub will be designed to obtain lower stress concentration, as shown in Figure 5.

2.3 Experimental Setup

The objective of this part is to test electric power output obtained from the FD2.7-500 wind turbine when connected with both our new wind turbine blade and the commercial blade. To obtain conditions of wind passing through our wind turbine blade, a specially designed translating frame has been fabricated and installed on a mini truck as shown in Figure 6.

The FD2.7-500 wind turbine set [8] consists of: a 3-phase 500 W synchronous generator, 3 blades with a length of 1.4 m and a root length of 0.15 m. The chord length at the tip and root of the wind turbine blades are 0.11 m and 0.2 m, respectively. The new wind turbine blades which will be described in the following section are installed to the FD2.7-500 wind turbine set using the 12 V and 24 V battery chargers. Steps for performance testing of the wind turbine blades are as follows: equipment associated with the wind turbine (i.e. current controller, 12 V battery, anemometer, and digital clamp multimeter) are installed on a mini truck, since the suitable wind tunnel is not locally available. The truck's velocity starts from the resting position and accelerates until achieving the simulated wind speed of 6–9 m/s. The truck is driven on a smooth surface of pavement on highway no. 2121, Thailand to ensure the simulated wind speed is maintained. When the blades are rotating with constant angular velocity, the potential difference (V) and the current (I) are recorded to determine the power output. After that, the 24 V battery is substituted with a 12 V battery and the testing is repeated.

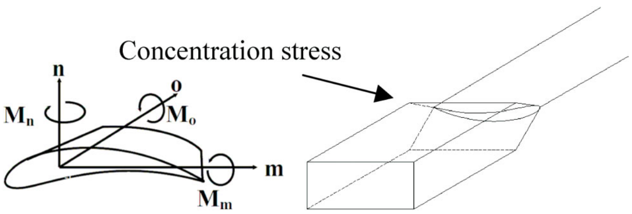

Figure 5. Stress concentration of new blade.

3. Results and Discussion

Following the method as shown in the flow chart in Figure 1, the appropriate shape of our new wind turbine can be determined by examining the tremendous net saving results as shown in Figure 7. The wind turbine blades

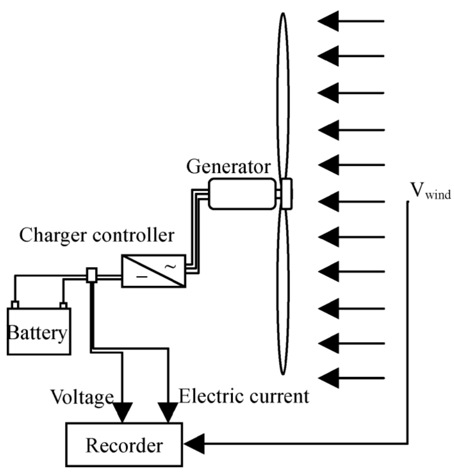

Figure 6. Illustration of wind turbine blade performance testing.

with the highest net saving (employed as the key indicator of our selection) at a life-time of 10 years is the blade with a length of 1.3 m, root length of 0.15 m, rotational speed of 180 rpm. The 3 blades have a chord length at the tip of the wind turbine of 0.06 m, chord length at the root of the wind turbine of 0.15 m, a pitch angle of 7°, and a non-twisted blade, with the power output of 235 W.

However, construction of this wind turbine blade shape cannot be locally constructed due to the oversize of the design. The new suitable wind turbine blade shape (NewB) is alternatively chosen in order to reduce the scale wind turbine blade and easier installation. From the simulation result, as shown in Figure 8, torque per blade area of our new blade obtained by using a new suitable wind turbine blade shape is only slightly different from the torque obtained by using the blade with the highest net saving determined above, the economic blade (EcoB), by 3.2 $N.m/m^2$ of the root mean squared error (RMSE). Moreover, power obtained by this type of new suitable wind turbine blade shape is relatively high compared to other blade types in simulation. With a new wind turbine parameter set, a turbine using 12 V and 24 V batteries

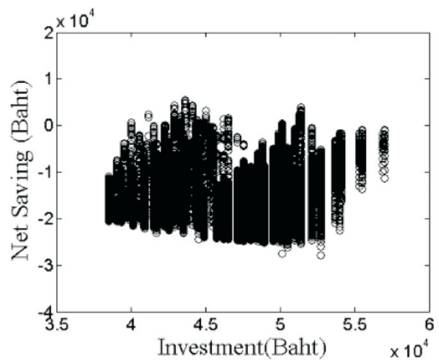

Figure 7. Simulation result.

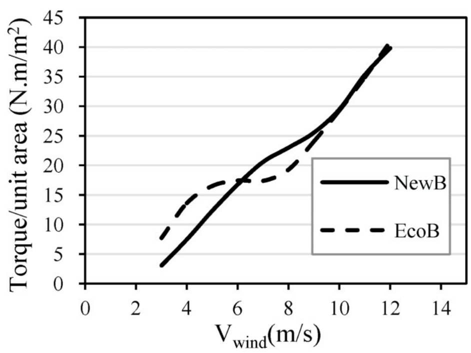

Figure 8. Relationship of wind velocity and Torque/blade.

charging or tip speed ratios of 2.3 and 3.14, respectively, high power and torque are achieved as shown in Figure 9.

The specifications of the 3 blades in the new wind turbine are as follows: a blade length of 1 m, a root length of 0.15 m, a constant chord length from the root to the tip of the wind turbine of 0.12 m, a pitch angle of 20° and a non-twisted blade. As shown in Figure 10, the simulation results of our newly designed blade are basically close to its experimental data with the standard deviation (STD) of ± 14%. The percentage of standard deviation used in this study is normalized with respect to the range of the experimental data. Figure 11 shows a comparison of the output torque per unit area (convert from power) of the commercial blade (ComB) with our newly designed blade. It is found from using the 12 V load system at wind velocities of 6 m/s and 9 m/s that powers generated from the new wind turbine blade are 48 W and 112 W and they are higher than the commercial wind turbine blade by 60% and 75%, respectively. This maybe because, at this rotational speed of 100 rpm, the high lift force coefficient can be obtained. Torque per unit area and energy is consequently high. Torque per unit area obtained from our new wind turbine blade at wind velocities of 6 m/s and 9 m/s is higher than that of the commercial wind turbine blade by 189% and 218%, respectively. However, when using the 24 V load system, our new wind turbine blade generates less power output than that of the commercial wind turbine blade by 17% and 32% at wind velocities of 6 m/s and 9 m/s, respectively. With the same wind velocity, the higher rotational speed of the blade, the higher relative velocity between the blade and the wind is. This is what is expected of a commercial wind turbine according to its design. However, our new

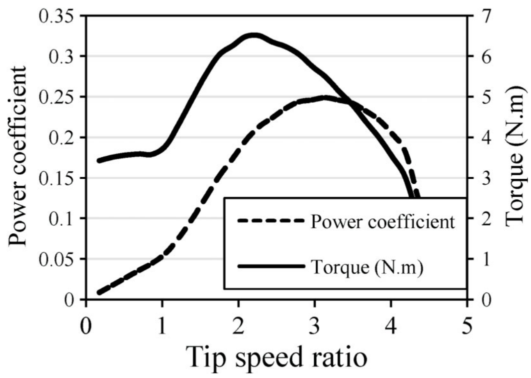

Figure 9. Simulation results of the new blade.

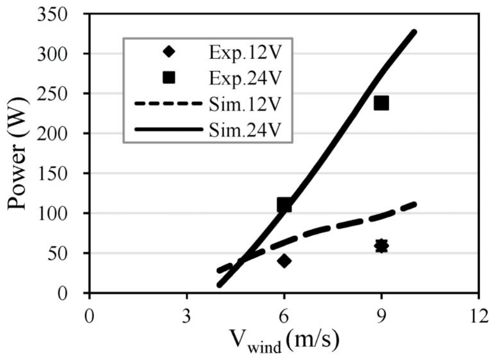

Figure 10. Comparison of simulation and experimental data.

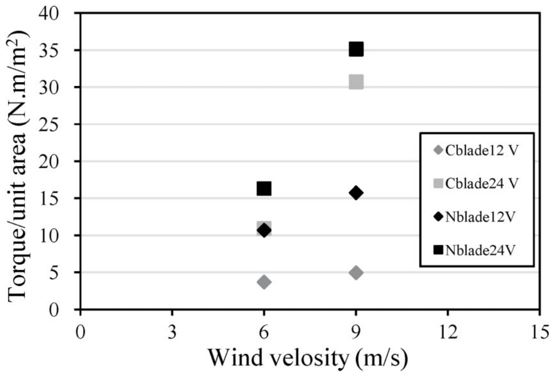

Figure 11. Testing result of both blade types.

wind turbine blade still generates higher torque per unit area in all wind speed operation. This implies that the wind turbine has easier operation starting. Especially, at a wind velocity of 6 m/s, our new wind turbine obtains a 27% efficiency while that of the commercial wind turbine is only 16%. Higher efficiency of our new wind turbine blade compared to that of commercial wind turbine blades resulted from suitable value selection of various parameters consistent with operating conditions; the airfoil's pitch angle has been adapted to have attack angle of which high C_L/C_D is obtained and its inertia is lower resulting from its lighter blade.

4. Conclusion

The simulation model based on the BEM theory has been successfully established. The new blade is designed according to the program results and is to be applied with the FD2.7-500 wind turbine for low wind speed operation of 6 m/s. It is found that, at a wind velocity of 6 m/s, the efficiency of the new wind turbine blade is 27% while that of the commercial wind turbine blade is only 16.5%. Good agreement between the experimental data and simulation results is achieved with STD of ± 14%.

Acknowledgements

This research was conducted under the collaboration Graduate School of Chiang Mai University Thailand with the strategic scholarships for frontier research network for the Post doctoral program, the office of the higher education commission. The authors are special thankful to Mr. Paul Lopez for the final proofreading.

Nomenclature

B	Number of blade
ρ	Air density (kg/m^3)
V_0	Wind velocity (m/s)
C_L	Lift coefficient
C_D	Drag coefficient
c	Chord (m)
R	Rotor radius (m)
a	Axial induction factor
a'	Tangential induction factor
ω	Rotational speed (rad/s)
λ	Local tip speed ration
C_N	Normal force coefficient
σ	Stress concentration (Pa)
N_s	Net saving
Cp	cost of electricity
A	Area (m^2)
H	annual time of operation (hrs/year)
P	power output of wind turbine
$C_{windturbine}$	overall cost of wind turbine
C_p	cost of electricity (Baht)
Q	power output of wind turbine (Wh)
Year	technical life of the wind turbine (yr)
D	deposit Rates (%)
R_v	resale value (%)
$C_{windturbine\_set}$	first cost of wind turbine (Baht)
$C_{windturbine\_blade}$	cost of manufacturing blade (Baht)
$C_{blade\_casting}$	cost of blade casting (Baht/m)
B_{chord}	chord factor
B_{twist}	blade twist factor
C_{blade_root}	cost of root casting (Baht)
$C_{coating}$	cost of mold coating (Baht/m)

References

[1] Information on http://www.dede.go.th.

[2] Chaichana, T. and Chaitep, S., "Wind Power Potential and Characteristic Analysis of Chiang Mai, Thailand," *Journal of Mechanical Science and Technology*, Vol. 24, pp. 1475–1479 (2010). doi: 10.1007/s12206-010-0415-3

[3] Clausen, P. D. and Wood, D. H., "Research and Development Issues for Small Wind Turbine," *Renewable Energy*, Vol. 16, pp. 922–927 (1999). doi: 10.1016/S0960-1481(98)00316-4

[4] Jonkman, J. M., "Modeling of the UAE Wind Turbine for Refinement of FAST_AD.," National Renewable Energy Laboratory, Colorado, U.S.A., Technical Report: NREL/TP-500-34755 (2003).

[5] Pathike, P., Katpradit, T., Terdtoon, P. and Chaitep, S., "Optimum Shape of Airfoil for Small Horizontal-Axis Wind Turbine," The Third International Conference on Science, Technology and Innovation for Sustainable Well-Being (STISWB III), Vietnam, Vol. 12–15, pp. 45–56 (2011).

[6] Buhl, M. L., "A New Empirical Relationship between Thrust Coefficient and Induction Factor for the Turbulent Windmill State," National Renewable Energy Laboratory, Colorado, U.S.A., Technical Report: NREL/TP-500-36834 (2005).

[7] Soylemez, M. S., "On the Thermoeconomical Optimization of Heat Pipe Heat Exchanger HPHE for Waste Heat Recovery," *Energy Conversion and Management*, Vol. 44, pp. 2509–2517 (2003). doi: 10.1016/S0196-8904(03)00007-4

[8] Information on http://www.engineo.co.th.

[9] Hansman, H. and Wismar, H., "Composite," ASM Handbook/Extraction Polyester Rasin, FB MVU, Werkstofftechnologie/Kunststofftechnik (2003).

Manuscript Received: Nov. 8, 2012
Accepted: May 18, 2013